Current noise geometrically generated by a driven magnet

Tim Ludwig,[1,2,3] Igor S. Burmistrov,[3,4] Yuval Gefen,[5] and Alexander Shnirman[2,6]
[1]*Institute for Theoretical Physics, Utrecht University, Princetonplein 5, 3584 CC Utrecht, The Netherlands*
[2]*Institut für Theorie der Kondensierten Materie, Karlsruhe Institute of Technology, 76128 Karlsruhe, Germany*
[3]*L.D. Landau Institute for Theoretical Physics RAS, Kosygina Street 2, 119334 Moscow, Russia*
[4]*Laboratory for Condensed Matter Physics, National Research University Higher School of Economics, 101000 Moscow, Russia*
[5]*Department of Condensed Matter Physics, Weizmann Institute of Science, 76100 Rehovot, Israel*
[6]*Institut für QuantenMaterialien und Technologien, Karlsruhe Institute of Technology, 76021 Karlsruhe, Germany*

(Received 17 June 2019; revised manuscript received 22 April 2020; accepted 23 April 2020; published 22 May 2020)

We consider a nonequilibrium cross-response phenomenon, where a driven magnetization gives rise to electric shot noise (but no d.c. current). This effect is realized on a nanoscale, with a small metallic ferromagnet which is tunnel coupled to two normal metal leads. The driving gives rise to a precessing magnetization. The geometrically generated noise is related to a nonequilibrium electron distribution in the ferromagnet. Our protocol provides a channel for detecting and characterizing ferromagnetic resonance.

DOI: 10.1103/PhysRevResearch.2.023221

I. INTRODUCTION

Off-diagonal (cross-)response phenomena, e.g., the thermoelectric effect, are ubiquitous in physics. In spintronic systems, by applying an electric charge current one can drive magnetization dynamics and vice versa [1–7]. This usually requires magnetic contacts or contacts with strong spin-orbit interaction (spin Hall effect) which allow for a conversion between spin and charge currents [8]. In this paper we report a higher order strongly nonequilibrium cross-response effect. Namely, we show that by driving magnetization dynamics one can generate electric shot noise [9,10] without generating charge current. Strikingly, neither magnetic leads nor spin Hall effect are needed and the leads can be at equilibrium with each other.

We consider a small metallic ferromagnet with a magnetization driven to precess. The ferromagnet is tunnel-coupled to two normal metal leads; see Fig. 1. The precessing magnetization drives the electrons of the ferromagnet into a strongly nonequilibrium state. This effect is most pronounced if the ferromagnet is small enough that internal relaxation is negligible compared to the relaxation due to the coupling to the leads. The precessing magnetization, in turn, induces nonequilibrium shot noise of the electric current. The nonequilibrium distribution responsible for the shot noise is governed by the geometric Berry phase due to the precession of the magnetization, branding the shot noise geometric. This shot noise exists even when both leads are in equilibrium with each other, although the average charge current vanishes then.

Shot noise is particularly interesting in spintronics because it gives insights into the magnetic configuration and its dynamics which may be hard to obtain otherwise [11–17].

II. RESULTS

To describe the magnetization dynamics we use the macrospin approximation; that is, the magnetization is described by a single vector $\boldsymbol{M} = M(\sin\theta\cos\phi, \sin\theta\sin\phi, \cos\theta)$. We assume that the magnetization precesses in a steady state, where polar angle θ and precession frequency $\dot{\phi}$ are constant. Under these assumptions, we find that the charge current vanishes on average, $I = 0$, but the current noise

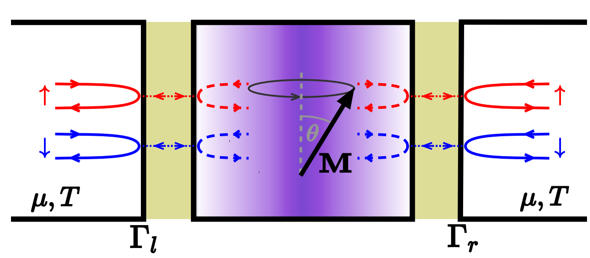

FIG. 1. A small metallic ferromagnet with precessing magnetization is tunnel coupled to two normal metal leads, which are at equilibrium with each other. The precessing magnetization pumps a spin-current from the small ferromagnet into the leads [4–6]. The average charge current vanishes by symmetry. Thus, the current of spin-up electrons and spin-down electrons balance each other on average and in each junction separately; in the ferromagnet, the precessing magnetization mixes spin-up and spin-down electrons. All four spin-resolved electron currents are fluctuating. These fluctuations combine to give rise to the noise of left to right (transport) charge current.

remains finite:

$$S = 4g_t T + g_t \sin^2\theta \left(\dot{\phi}\, \coth\frac{\dot{\phi}}{2T} - 2T\right). \quad (1)$$

Here $g_t = 2(\rho_\uparrow + \rho_\downarrow)\Gamma_l\Gamma_r/(\Gamma_l + \Gamma_r)$ is the total conductance of the double tunnel junction, where ρ_σ is the magnet's spin-dependent density of states. The rates Γ_l and Γ_r characterize the spin-conserved tunneling to the left and right lead, respectively.

At high temperatures ($T \gg \dot{\phi}$), the noise is dominated by the first term $S \approx 4g_t T$, which is the standard thermal noise. At low temperatures ($T \ll \dot{\phi}\sin^2\theta$), however, the noise is dominated by the second term $S \approx g_t \sin^2\theta\, |\dot{\phi}|$. Interestingly, in both limits (high and low temperature) our results agree with those for a single tunnel junction [16]. For intermediate temperatures, however, we obtain a different result for the charge current noise. This difference arises from the nonequilibrium distribution which develops in the small magnet; see Fig. 2.

The origin of charge current noise can be understood as follows. As a special case of spin pumping [4–6], the precessing macrospin assists electrons in tunneling between magnet and leads. This macrospin assisted tunneling drives the electron system into a strong nonequilibrium state [18,19]. As the macrospin dynamics is the source of driving for the electron system, it governs the resulting nonequilibrium distribution, Fig. 2. In turn, the macrospin dynamics governs the nonequilibrium noise of charge current, Eq. (1), where the precession frequency $\dot{\phi}$ acts similar to the voltage bias for standard shot noise.

In the following, we provide the details of this argument to derive our main result, Eq. (1). Finally, we show that this result can be useful to detect and characterize magnetization dynamics, Fig. 3.

III. DERIVATION OF CURRENT NOISE

A. Macrospin assisted tunneling

The precessing macrospin (magnetization) makes the magnet's Hamiltonian time dependent and, thereby, it affects the tunneling of electrons between magnet and leads. To understand this effect, it is sufficient to start from the case of coupling to only one, e.g., left, lead.

For the electrons in the magnet the magnetization $\boldsymbol{M}(t)$ acts as a magnetic field. We assume the electrons to be noninteracting. In turn, the magnet can be described by a single-particle Hamiltonian, while the many-particle information is contained in the electron distribution. So, the magnet's full Hamiltonian is given by $H_m = \sum_{a\sigma\sigma'} |a\sigma\rangle h_{m,a}^{\sigma\sigma'}\langle a\sigma'|$ with $h_{m,a} = \epsilon_a - \boldsymbol{M}(t)\,\boldsymbol{\sigma}/2$, where $\boldsymbol{\sigma} = (\sigma_x, \sigma_y, \sigma_z)$ is the vector of Pauli-matrices, a denotes orbital states in the magnet with energy ϵ_a, and σ denotes eigenvalues of σ_z. We assume spin-conserved tunneling to the (left) lead with tunnel amplitude t_l. This process is described by $H_t = \sum_{a\nu\sigma} |a\sigma\rangle t_l \langle\nu\sigma| + \text{h.c.}$, where ν denotes the states in the (left) lead. We neglect possible dependence of the tunneling amplitudes t_l, t_l^* on the states a, ν [20]. The electrons in the (left) lead are assumed to be noninteracting $H_l = \sum_{\nu\sigma} |\nu\sigma\rangle\epsilon_\nu\langle\nu\sigma|$.

To determine the tunneling rates between states in the magnet and states in the lead, we want to use Fermi's Golden Rule, where the tunneling Hamiltonian is treated as perturbation. However, there is a problem: to apply Fermi's Golden Rule, the unperturbed Hamiltonian must be *time independent*; which is not the case, due to the precessing macrospin. In order to circumvent this obstacle, we transfer to the magnetization's rotating frame of reference. Formally, this is achieved by applying the transformation $U(t) = \sum_{a\sigma} |a\sigma; \boldsymbol{m}(t)\rangle\langle a\sigma| + \sum_{\nu\sigma} |\nu\sigma\rangle\langle\nu\sigma|$, where $\boldsymbol{m} = \boldsymbol{M}/M$ and $|a\sigma; \boldsymbol{m}(t)\rangle$ is an instantaneous eigenstate of $\boldsymbol{m}(t)\hat{\boldsymbol{\sigma}}$; that is, $\boldsymbol{m}(t)\hat{\boldsymbol{\sigma}}|a\sigma; \boldsymbol{m}(t)\rangle = \sigma|a\sigma; \boldsymbol{m}(t)\rangle$, where $\hat{\boldsymbol{\sigma}}/2$ is the spin-1/2 operator. This transformation leaves the lead's Hamiltonian unaffected, $\tilde{H}_l := UH_lU^\dagger = H_l$, but it diagonalizes the magnet's Hamiltonian $\tilde{H}_m := UH_mU^\dagger = \sum_{a\sigma} |a\sigma\rangle\tilde{h}_{m,a}^{\sigma\sigma}\langle a\sigma|$, where $\tilde{h}_{m,a} = \epsilon_a - M\sigma_z/2$ is diagonal in spin space and independent of time. The transformation also affects the tunneling Hamiltonian $\tilde{H}_t = UH_tU^\dagger = \sum_{a\nu\sigma\sigma'} |a\sigma\rangle[R^\dagger(t)]_{\sigma\sigma'} t_l\langle\nu\sigma'| +$ h.c.. Effectively, the tunneling amplitude becomes spin and time dependent,

$$t_l \longrightarrow R^\dagger(t)\, t_l, \quad (2)$$

where $R(t)$ is a spin-space rotation defined via $[R(t)]_{\sigma\sigma'} = \langle a\sigma; \boldsymbol{m}(t)|a\sigma'\rangle$. Besides rotating the Hamiltonian, a time-dependent transformation generates a new term $-i\,U\dot{U}^\dagger = -i\sum_{a\sigma\sigma'} |a\sigma\rangle[R^\dagger\dot{R}]_{\sigma\sigma'}\langle a\sigma'|$ in the Hamiltonian of the system in the rotating reference frame.

To proceed, we choose an Euler-angle representation for the rotation, $R(t) = e^{-i\phi\sigma_z/2}e^{-i\theta\sigma_y/2}e^{i(\phi-\chi)\sigma_z/2}$, where we introduce an angle χ that is a gauge variable, see Ref. [21]. In turn, the new term becomes $-iR^\dagger\dot{R} = [\dot{\phi}(1-\cos\theta) - \dot{\chi}]\sigma_z/2 \; + e^{i\chi\sigma_z}[\dot{\phi}\sin\theta\sigma_x/2]e^{i\phi\sigma_z}$. Its spin-off-diagonal part (the second contribution) induces (Landau-Zener) transitions between spin-up and spin-down states. However, assuming M to be large, these transitions can be disregarded [21]. For $\chi = 0$, the remaining spin-diagonal part (the first term) gives rise to an additional time-evolution phase, the so-called *geometrical Berry -phase*, which is acquired because of the magnetization dynamics. However, following Ref. [21], we choose $\dot{\chi} = \dot{\phi}(1-\cos\theta)$ to eliminate the remaining spin-diagonal part of $-iR^\dagger\dot{R}$. This trick with the proper choice of χ allows us to exclude the term $-i\,U\dot{U}^\dagger$ in the Hamiltonian in the rotating frame of reference from the analysis. This might come as a surprise, because the Berry phase is a physical phase and, thus, it cannot be eliminated. And indeed, for a proper derivation of the magnetization dynamics we would have to be more careful with the choice of gauge [21]. But even here—where the magnetization dynamics is assumed to be given—the Berry phase remains relevant. By the choice of gauge, it is shifted to the tunneling amplitude, Eq. (2).

Now, it has become straightforward to determine the rate for macrospin assisted tunneling. We consider $\tilde{H}_m + \tilde{H}_l$ as unperturbed Hamiltonian, whereas the tunneling Hamiltonian $\tilde{H}_t$ is treated perturbatively. Using Fermi's golden rule, we obtain the rate for macrospin assisted tunneling between a state in the left lead $|\nu\sigma'\rangle$ and a state in the magnet $|a\sigma\rangle$,

$$\Gamma^l_{\nu\sigma'\leftrightarrow a\sigma} = \pi|t_l|^2(1 + \sigma\sigma'\cos\theta)\,\delta(\xi_{a\sigma} - \epsilon_\nu + \sigma'\omega_{\sigma\sigma'}), \quad (3)$$

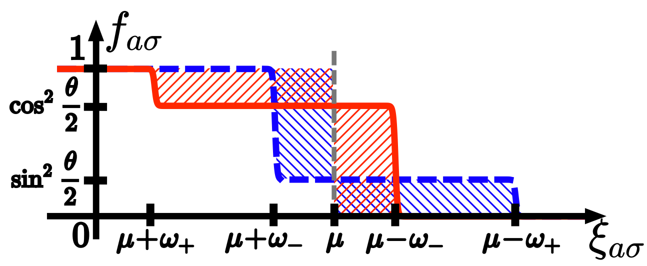

FIG. 2. The magnet's electron distribution (filling factor) is shown for spin-up (red solid) and spin-down (blue dashed). The four shaded areas are all equal in size: $\sin^2\theta\,|\dot\phi|/4$. It means that electrons are redistributed in energy space such that the magnetization length M remains constant. Plot parameters: $\theta=\pi/3$ and $\dot\phi<0$.

where $\xi_{a\sigma}=\epsilon_a-M\sigma/2$ is the energy of an electron in the state $|a\sigma\rangle$. The energy shift $\omega_{\sigma\sigma'}=\dot\phi(1-\sigma\sigma'\cos\theta)/2$ arises from the time-dependence of the rotating-frame tunneling amplitudes, Eq. (2), which include the rotations $[R(t)]_{\sigma\sigma'}=\frac{1+\sigma'-\sigma+\sigma\sigma'}{2}\sqrt{(1+\sigma\sigma'\cos\theta)/2}\,e^{-i\sigma\omega_{\sigma\sigma'}t}$. Physically, the precessing macrospin acts as a time-dependent magnetic field for the electrons. Thus it can give energy to—or take energy from—electrons that tunnel between lead and magnet. So, as a special case of spin pumping [4–6], the precessing macrospin assists electrons in tunneling.

B. Strongly nonequilibrium distribution

The tunneling rate (3) alone is not enough in order to compute the transport via the tunnel junction. Via the macrospin assisted tunneling, the precessing magnetization drives electrons in the magnet away from equilibrium. The resulting nonequilibrium distribution (calculated in the rotating frame of reference) is characterized by the filling factor $f_{a\sigma}$, which gives the probability to find an electron in a state $|a\sigma\rangle$. The filling factor is governed by the master equation

$$\dot f_{a\sigma}=\Gamma^{(\mathrm{in})}_{a\sigma}-\Gamma^{(\mathrm{out})}_{a\sigma}\,, \tag{4}$$

where $\Gamma^{(\mathrm{in})/(\mathrm{out})}_{a\sigma}$ is the total tunneling rate *into*/*out of* the state $|a\sigma\rangle$.

Knowing the macrospin assisted tunneling rate, Eq. (3), we can straightforwardly determine the total *in*- and *out*-rates. But before doing so, we bring the second (right) lead back into the problem. The right lead is assumed to be similar to the left lead. The only differences are the right lead's states $\tilde\nu$, their energies $\epsilon_{\tilde\nu}$, and the tunneling amplitude t_r. Consequently, the tunneling rate between the right lead and the magnet, $\Gamma^r_{\tilde\nu\sigma'\leftrightarrow a\sigma}$,can be obtained from Eq. (3) after the replacements $t_l\to t_r$ and $\nu\to\tilde\nu$.

It is now straightforward to write down the total in- and out-rates as a sum over the left and right leads. The total in-rate is given by $\Gamma^{(\mathrm{in})}_{a\sigma}=\gamma^{(\mathrm{in})}(1-f_{a\sigma})$, where $\gamma^{(\mathrm{in})}=\gamma^{(\mathrm{in})}_l+\gamma^{(\mathrm{in})}_r$ with $\gamma^{(\mathrm{in})}_l=\sum_{\nu\sigma'}\Gamma^l_{\nu\sigma'\leftrightarrow a\sigma}f_l(\epsilon_\nu)$ and similarly for the right lead. As usual, the factor $(1-f_{a\sigma})$ is responsible for the Pauli principle; an electron can tunnel into the state $|a\sigma\rangle$, only if this state is empty. For an electron to tunnel from the state $|\nu\sigma\rangle$ or $|\tilde\nu\sigma\rangle$ that state must be filled; this explains the appearance of the leads' distribution functions $f_{l,r}$ in the expression for $\Gamma^{(\mathrm{in})}_{a\sigma}$. The total out-rate is determined analogously, only the roles of $f_{a\sigma}$ and $f_{l,r}$ are reversed: $\Gamma^{(\mathrm{out})}_{a\sigma}=\gamma^{(\mathrm{out})}f_{a\sigma}$, where $\gamma^{(\mathrm{out})}=\gamma^{(\mathrm{out})}_l+\gamma^{(\mathrm{out})}_r$ with $\gamma^{(\mathrm{out})}_l=\sum_{\nu\sigma'}\Gamma^l_{\nu\sigma'\leftrightarrow a\sigma}[1-f_l(\epsilon_\nu)]$ and similarly for the right lead.

We are particularly interested in the long-time limit; that is, when a stationary distribution has developed in the small magnet. Thus, we set $\dot f_{a\sigma}=0$ in Eq. (4) and obtain

$$f_{a\sigma}=\cos^2\frac{\theta}{2}f(\xi_{a\sigma}+\sigma\omega_-)+\sin^2\frac{\theta}{2}f(\xi_{a\sigma}-\sigma\omega_+), \tag{5}$$

where $\omega_\pm=\dot\phi(1\pm\cos\theta)/2$ arises from $\omega_{\sigma\sigma'}$ for $\sigma'=\mp\sigma$. Furthermore, we assumed that both leads are in equilibrium with each other $f_{l,r}(\omega)=f(\omega)=1/[e^{\beta(\omega-\mu)}+1]$. Also we neglected the energy dependence of the leads' densities of states $\rho_{l,r}$. The established magnet's electron distribution (filling factor), Eq. (5), is clearly different for the two spin species and, at low temperatures, it is not even close to a Fermi distribution; see Fig. 2. In other words, macrospin assisted tunneling induces a strongly nonequilibrium electron distribution in the magnet.

The emerging nonequilibrium distribution, Eq. (5), is governed by the geometrical Berry phase [22]. Namely, ω_- is the rate at which the Berry phase is acquired and ω_+ is related to it by $\omega_+=\dot\phi-\omega_-$. In other words, the distribution's nonequilibrium features have their origin in the geometric Berry phase. Because the noise of charge current is intimately linked to these nonequilibrium features, we refer to it as geometrically generated noise.

C. Noise of charge current

The noise of charge current is determined by the statistics of charge transport. In our noninteracting model, the charge transport can be considered separately for each single particle state $|a\sigma\rangle$. Then, the total average current is given by the sum $I=\sum_{a\sigma}I_{a\sigma}$, where $I_{a\sigma}$ is the average current which is transported through the state $|a\sigma\rangle$. Analogously, the total noise of charge current is given by the sum $S=\sum_{a\sigma}S_{a\sigma}$.

To find $I_{a\sigma}$ and $S_{a\sigma}$, we study the statistics of the number of electrons $n_{a\sigma}$ which entered the state $|a\sigma\rangle$ through the left junction. Electrons leaving through the left junction are counted negatively. At low frequency, it is sufficient to focus on the transport through one junction: as the magnet cannot store additional charges for a long time, charge conservation demands the charge current to be equal in both junctions. The same holds for the noise of the charge current. So, the average $\langle n_{a\sigma}\rangle$ determines the current $I_{a\sigma}=\partial_t\langle n_{a\sigma}\rangle$ and the cumulant $\langle\langle n^2_{a\sigma}\rangle\rangle$ determines the noise $S_{a\sigma}=2\,\partial_t\langle\langle n^2_{a\sigma}\rangle\rangle$.

The probability that $n_{a\sigma}$ electrons entered the state $|a\sigma\rangle$ through the left junction is convenient to present in the following form: $P_{a\sigma}(n_{a\sigma})=F_{a\sigma}(n_{a\sigma})+\bar F_{a\sigma}(n_{a\sigma})$. Here, $F_{a\sigma}(n_{a\sigma})$ is the probability that the state $|a\sigma\rangle$ is occupied and $n_{a\sigma}$ electrons have tunneled through the left junction. Analogously, $\bar F_{a\sigma}(n_{a\sigma})$ is the probability that the state $|a\sigma\rangle$ is empty and $n_{a\sigma}$ electrons have tunneled through the left junction. The probabilities $F_{a\sigma}(n_{a\sigma})$ and $\bar F_{a\sigma}(n_{a\sigma})$ are governed by master equations similar to the one given by Eq. (4). We only have to keep track for changing $n_{a\sigma}$ by 1 in the course of an electron tunneling through the left junction. So, the corresponding master equations are given by

$$\dot{F}(n) = \gamma_l^{(\mathrm{in})}\bar{F}(n-1) + \gamma_r^{(\mathrm{in})}\bar{F}(n) - \gamma^{(\mathrm{out})}F(n),$$
$$\dot{\bar{F}}(n) = \gamma_l^{(\mathrm{out})}F(n+1) + \gamma_r^{(\mathrm{out})}F(n) - \gamma^{(\mathrm{in})}\bar{F}(n). \qquad (6)$$

Here and in the following, we suppress indices $a\sigma$ in all quantities to simplify the notation.

In order to solve the master equation (6) and compute the average current and noise it is convenient to make a Fourier transform. In other words, instead of directly focusing on the probabilities $F(n)$ and $\bar{F}(n)$, it is more convenient to consider the moment generating functions $\chi_F(\lambda) = \sum_n F(n)e^{-i\lambda n}$ and $\chi_{\bar{F}}(\lambda) = \sum_n \bar{F}(n)e^{-i\lambda n}$, where we also suppress indices $a\sigma$ for the generating functions $\chi_{F,\bar{F}}$ and the, so called, counting field λ. Then the Fourier transform of Eq. (6) becomes

$$\begin{pmatrix}\dot{\chi}_F \\ \dot{\chi}_{\bar{F}}\end{pmatrix} = \begin{pmatrix} -\gamma^{(\mathrm{out})} & e^{-i\lambda}\gamma_l^{(\mathrm{in})} + \gamma_r^{(\mathrm{in})} \\ e^{i\lambda}\gamma_l^{(\mathrm{out})} + \gamma_r^{(\mathrm{out})} & -\gamma^{(\mathrm{in})}\end{pmatrix}\begin{pmatrix}\chi_F \\ \chi_{\bar{F}}\end{pmatrix}. \qquad (7)$$

We note that Eq. (7) has the form familiar from the counting statistics of a metallic island coupled to two reservoirs [23]. However, we emphasize that the generalized master equation (7) are governed by the macrospin-assisted tunneling-rate, Eq. (3), which was calculated in the magnetization's rotating frame of reference.

The matrix appearing on the right-hand side of Eq. (7) has the eigenvalues

$$E_{a\sigma}^{\pm}(\lambda) = -(\gamma^{(\mathrm{in})} + \gamma^{(\mathrm{out})})/2 \pm \big[(\gamma^{(\mathrm{in})} + \gamma^{(\mathrm{out})})^2/4 + (e^{-i\lambda} - 1)\gamma_l^{(\mathrm{in})}\gamma_r^{(\mathrm{out})} + (e^{i\lambda} - 1)\gamma_r^{(\mathrm{in})}\gamma_l^{(\mathrm{out})}\big]^{1/2}. \qquad (8)$$

These eigenvalues determine the time evolution of $\chi_F(\lambda)$ and $\chi_{\bar{F}}(\lambda)$. At low frequencies (long times), the generating functions are dominated by the smaller eigenvalue; more precisely, $\lim_{t\to\infty} \ln[\chi_F(\lambda) + \chi_{\bar{F}}(\lambda)]/t = E_{a\sigma}^{+}(\lambda)$. So, the state-resolved average charge current and its noise are given by

$$I_{a\sigma} = i\partial_\lambda E_{a\sigma}^{+}(\lambda)|_{\lambda=0}, \quad S_{a\sigma} = 2(i\partial_\lambda)^2 E_{a\sigma}^{+}(\lambda)|_{\lambda=0}. \qquad (9)$$

For the constant leads' densities of states $\rho_{l,r}$, the state-resolved average current vanishes, $I_{a\sigma} = (\gamma_l^{(\mathrm{in})}\gamma_r^{(\mathrm{out})} - \gamma_r^{(\mathrm{in})}\gamma_l^{(\mathrm{out})})/(\gamma^{(\mathrm{in})} + \gamma^{(\mathrm{out})}) = 0$. Consequently, the total average current vanishes $I = \sum_{a\sigma} I_{a\sigma} = 0$ as one might expect from symmetry. However, the noise remains. Using Eq. (9), we obtain $S_{a\sigma} = 2(\gamma_l^{(\mathrm{in})}\gamma_r^{(\mathrm{out})} + \gamma_r^{(\mathrm{in})}\gamma_l^{(\mathrm{out})})/(\gamma^{(\mathrm{in})} + \gamma^{(\mathrm{out})})$. Now, we define $\Gamma_l = \pi|t_l|^2\rho_l$ and $\Gamma_r = \pi|t_r|^2\rho_r$, and we assume the spin-resolved magnet's density of states $\rho_{\uparrow,\downarrow}$ to be constant on all scales smaller than M. Then, summing over all states, $S = \sum_{a\sigma} S_{a\sigma}$, yields our main result, Eq. (1).

IV. APPLICATION TO FMR-DRIVEN MAGNET

Now let us consider our setup under conditions of a ferromagnetic resonance (FMR). The dynamics of the magnetization is phenomenologically described by the Landau-Lifshitz-Gilbert equation $\dot{\boldsymbol{m}} = \boldsymbol{m} \times \boldsymbol{B} - \alpha\, \boldsymbol{m} \times \dot{\boldsymbol{m}}$, with the magnetization direction $\boldsymbol{m} = \boldsymbol{M}/M$ and the Gilbert-damping coefficient α. For negligible internal relaxation, the damping is dominated by the coupling to the leads. For the FMR setup, we choose the magnetic field $\boldsymbol{B} = (\Omega\cos\omega_d t, \Omega\sin\omega_d t, B_0)$ with a fixed component B_0 in the z direction and, perpendicular to it, a small driving field with strength Ω and frequency ω_d. Without driving ($\Omega = 0$), the Gilbert-damping would relax the magnetization towards $\theta = 0$. With driving ($\Omega \neq 0$), however, the magnetization can be brought into a steady state precession. That is, after the decay of transient effects, the magnetization precesses at the frequency of the driving field $\dot{\phi} = \omega_d$ and the polar angle θ is determined by the competition between Gilbert-damping and FMR driving. Explicitly, θ is determined by

$$\sin^2\theta = \frac{(\Omega_+ + \Omega_-)^2}{\Omega_+^2 + \Omega_-^2 + 2\Delta^2 + 2\sqrt{(\Delta^2 + \Omega_+^2)(\Delta^2 + \Omega_-^2)}}, \qquad (10)$$

with $\Omega_\pm = \Omega \pm \alpha\omega_d$ and the detuning parameter $\Delta = \omega_d + B_0$. The dependence of $\sin^2\theta$ on precession frequency ω_d has a resonant character with a maximum at $\omega_d = -B_0$. This ferromagnetic resonance of the magnetization's steady state precession directly translates into a resonance in the current noise; see Fig. 3. At low temperatures, $T \ll \omega_d \sin^2\theta$, the form of the resonance in the current noise resembles the FMR structure of the stationary precession angle. At higher temperatures, the resonance in the current noise can be visible on top of the constant thermal noise.

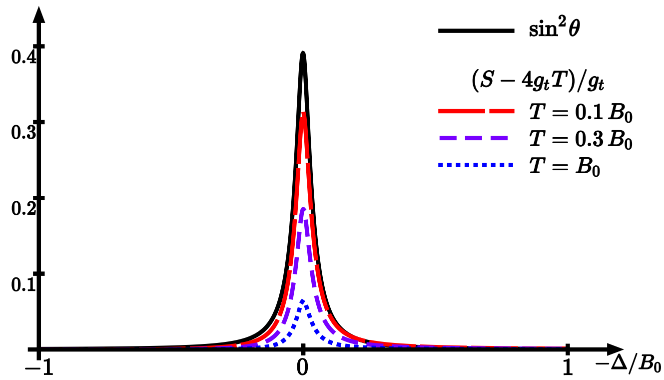

FIG. 3. When the steady state precession of the magnetization is maintained by driving with a FMR setup, the polar angle θ depends on driving frequency $\dot{\phi} = \omega_d$. The peak of $\sin^2\theta$ at $\omega_d = -B_0$ ($\Delta = 0$) is a typical FMR peak. We show the zero-frequency noise of charge current that is generated by the precessing magnetization; we subtract the thermal contribution and normalize onto the value of the total conductance, that is, we show $(S - 4g_t T)/g_t$. The geometrically generated noise of charge current clearly reflects the peak structure of $\sin^2\theta$ in the FMR setup. Parameters in figure: $\alpha = 0.04$, $\Omega/(\alpha B_0) = 0.63$.

V. CONCLUSION

We have found a higher order nonequilibrium off-diagonal response effect. Namely, we have shown that zero-frequency shot noise of charge current is generated by a precessing magnetization of a small magnet which it is tunnel coupled to two normal metal leads. This noise, Eq. (1), crucially depends on the electronic distribution function which is, in turn, geometrically governed by the magnetization dynamics; see Fig. 2. Thus, the noise of the charge current, Eq. (1), is generated by the precessing magnetization. For the FMR setup, Fig. 3, this effect can be used to detect the magnetization dynamics in spite of the vanishing average charge current.

ACKNOWLEDGMENTS

We thank G. E. W. Bauer, R. A. Duine, M. Keßler, and W. Wulfhekel for fruitful discussions. This work was supported by DFG Research Grant No. SH 81/3-1. The research of T.L. is partially supported by the Russian Foundation for Basic Research under the Grant No. 19-32-50005. Furthermore, T.L. acknowledges KHYS of KIT and the Feinberg Graduate school of WIS for supporting a stay at WIS; I.S.B. acknowledges partial support by the Alexander von Humboldt Foundation and the Basic research program of HSE; Y.G. acknowledges the DFG Research Grant RO 2247/11-1 and the Italy- Israel cooperation project QUANTRA.

[1] J. C. Slonczewski, J. Magn. Magn. Mater. **159**, L1 (1996).
[2] L. Berger, Phys. Rev. B **54**, 9353 (1996).
[3] L. Berger, Phys. Rev. B **59**, 11465 (1999).
[4] Y. Tserkovnyak, A. Brataas, and G. E. W. Bauer, Phys. Rev. Lett. **88**, 117601 (2002).
[5] A. Brataas, Y. Tserkovnyak, G. E. W. Bauer, and B. I. Halperin, Phys. Rev. B **66**, 060404(R) (2002).
[6] Y. Tserkovnyak, A. Brataas, G. E. W. Bauer, and B. I. Halperin, Rev. Mod. Phys. **77**, 1375 (2005).
[7] Y. Tserkovnyak, T. Moriyama, and J. Q. Xiao, Phys. Rev. B **78**, 020401(R) (2008).
[8] See however: M. Jonson, R. Shekhter, O. Entin-Wohlman, A. Aharony, H. Park, and D. Radić, Phys. Rev. B **100**, 115406 (2019).
[9] R. Landauer, Nature (London) **392**, 658 (1998).
[10] Y. M. Blanter and M. Büttiker, Phys. Rep. **336**, 1 (2000).
[11] J. Foros, A. Brataas, G. E. W. Bauer, and Y. Tserkovnyak, Phys. Rev. B **79**, 214407 (2009).
[12] T. Arakawa, J. Shiogai, M. Ciorga, M. Utz, D. Schuh, M. Kohda, J. Nitta, D. Bougeard, D. Weiss, T. Ono, and K. Kobayashi, Phys. Rev. Lett. **114**, 016601 (2015).
[13] A. Kamra and W. Belzig, Phys. Rev. B **94**, 014419 (2016).
[14] A. Kamra and W. Belzig, Phys. Rev. Lett. **116**, 146601 (2016).
[15] J. P. Cascales, D. Herranz, U. Ebels, J. A. Katine, and F. G. Aliev, Appl. Phys. Lett. **107**, 052401 (2015).
[16] P. Virtanen and T. T. Heikkilä, Phys. Rev. Lett. **118**, 237701 (2017).
[17] B. Horovitz and A. Golub, Phys. Rev. B. **99**, 241407(R) (2019).
[18] T. Ludwig, I. S. Burmistrov, Y. Gefen, and A. Shnirman, Phys. Rev. B **95**, 075425 (2017).
[19] T. Ludwig, I. S. Burmistrov, Y. Gefen, and A. Shnirman, Phys. Rev. B **99**, 045429 (2019).
[20] Formally, one should treat ν as a collective index $\nu = (n, k)$, which denotes the transport channel n and the momentum k. The tunneling amplitudes would depend on the channel index and the state in the magnet $t_{l,an}$, $t^*_{l,an}$; however, this dependence can be disregarded for a large number of transport channels that are weakly and randomly coupled to the states in the magnet; for details see Ref. [18].
[21] A. Shnirman, Y. Gefen, A. Saha, I. S. Burmistrov, M. N. Kiselev, and A. Altland, Phys. Rev. Lett. **114**, 176806 (2015).
[22] This might seem surprising, as we have eliminated the Berry phase from $-iR^\dagger\dot{R}$ by a specific choice of gauge χ. However, the Berry phase is a physical phase. Thus, being eliminated from $-iR^\dagger\dot{R}$, it must show up in a different place, which is the rotating-frame tunneling Hamiltonian $\tilde{H}_t$. In turn, the Berry phase enters the macrospin assisted tunneling rate, Eq.(3), and consequently it governs the nonequilibrium features of the distribution, Eq. (5).
[23] M. Esposito, U. Harbola, and S. Mukamel, Rev. Mod. Phys. **81**, 1665 (2009).